Crystal Structure and Magnetic Properties of $Bi(Bi_9)[NbCl_6]_3$, a New Member of the Structure Family $Bi(Bi_9)[MX_6]_3$, and the Crystal Structure of $Bi_8[Ta_2O_2Br_7]_2$

Johannes Beck*[a] and Tobias Hilbert[a]

Keywords: Bismuth / Niobium / Tantalum / Magnetic properties / X-ray diffraction

Bi and Bi^{III} halides comproportionate to form subvalent cationic Bi clusters of various size and shape that can be stabilized in the solid state in the presence of suitable complex ions. Transition metal chlorides and bromides of group 4 elements lead to compounds of the $Bi(Bi_9)[MX_6]_3$ family, of which all members with M = Zr, Hf; X = Cl, Br are known. At 550 K Bi, $BiCl_3$ and $NbCl_5$, surprisingly, yield the isotypic $Bi^+(Bi_9^{5+})([NbCl_6]^{2-})_3$ containing Nb^{IV} formed by reduction of Nb^V. The crystal structure [hexagonal; $P6_3/m$; a = 1377.1(2), c = 1065.5(2) pm; Z = 2] contains Bi_9^{5+} clusters, octahedral $[NbCl_6]^{2-}$ and disordered Bi^+ ions. The low, temperature-dependent paramagnetic moment (76 K: 0.99 B.M.; 295 K: 1.22 B.M.) confirms the reduction of Nb to the +IV state. $Bi_8[Ta_2O_2Br_7]_2$, formed by a trace of H_2O in a reaction of Bi, $BiBr_3$ and $TaBr_5$ at 570 K, adopts a new structure type [tetragonal; $P4/mnc$; a = 1448.0(1), c = 1830.6(2) pm; Z = 4] and consists of square-antiprismatic Bi_8^{2+} clusters and one-dimensional polymeric bromooxotantalate(V) anions.

Introduction

Bismuth was one of the first elements for which subvalent species with oxidation states between 0 and +III were studied systematically. The series of discrete, homonuclear cations Bi^+, Bi_2^{4+}, Bi_3^+, Bi_5^+, Bi_5^{3+}, Bi_6^{2+}, Bi_8^{2+}, and Bi_9^{5+} has made bismuth the classical example of naked clusters among the main group elements. Because of these exceptional properties bismuth has been called "The Wonder Metal".[1] The tricapped trigonal-prismatic Bi_9^{5+} is the largest known molecular cluster of bismuth. It was first characterized in the binary subchloride Bi_6Cl_7 together with polymeric chlorobismuthate(III) anions of composition $[Bi_3Cl_{14}]^{5-}$,[2,3] and later also in the ternary phase $Bi(Bi_9)[HfCl_6]_3$.[4] With tetrachloroaluminate counterions bismuth tends to form smaller clusters such as the square-antiprismatic Bi_8^{2+} in $Bi_8[AlCl_4]_2$ [3,5,6] and the trigonal-bipyramidal Bi_5^{3+} in $Bi_5[AlCl_4]_3$.[5,7] Subsequent studies focused on replacing $[AlCl_4]^-$ with other anions and led to the preparation of several compounds like Bi_6Br_7,[8] $Bi(Bi_9)[ZrBr_6]_3$,[9] $Bi(Bi_9)[ZrCl_6]_3$ [10] and $Bi_5[GaCl_4]_3$.[11] New clusters, Bi_2^{4+} in $Bi_2[M_4X_8]$ (M = Al, Ga; X = S, Se)[12] and Bi_5^+/Bi_6^{2+} in $Bi_{34}Ir_3Br_{37}$ [13] were found in the thus far unexplored ternary systems.

Numerous articles deal with theoretical approaches to explain the bonding situation in these predominantly deltahedral clusters. The structures of Bi_5^{3+} and Bi_8^{2+} can be understood as *closo* and *arachno* clusters that fulfill Wade's rules.[14] The nine-atomic Bi_9^{5+} shows substantial deviation from the predicted structure of a monocapped square antiprism, which is adopted by the isoelectronic Zintl ion Sn_9^{4-}.[15] The actual three-capped trigonal-prismatic structure is related to a *closo* structure. Elongation along the threefold axis is the result of the antibonding character of the HOMO. The molecular geometries and electron configuration of different main group element clusters have been compared in several reviews.[16,17] The high degree of electron delocalization in the polyhedral clusters was recently termed "three-dimensional" or "spherical" aromaticity.[18,19]

We intended to expand the structure family $Bi(Bi_9)[MX_6]_3$ and to obtain new structure types by a varied cation/anion ratio using anions with a lower charge. We chose $NbCl_5$ as Lewis acid, since hexachloroniobates(V) are suitable for stabilizing naked clusters such as chalcogen polycations.[20,21] Thus, a compound composed of polycationic Bi clusters and $[NbCl_6]^-$ ions was expected. Instead, $Bi^+(Bi_9^{5+})([NbCl_6]^{2-})_3$ was obtained under reduction to Nb^{IV}. A special feature of this structure type of the general formula $Bi(Bi_9)[MX_6]_3$ is the occurrence of Bi^+ ions as a one-dimensional chain in a wide channel made up of $[MX_6]^{2-}$ anions. Alternative split-position models for these one-dimensionally disordered Bi^+ ions will be discussed. Finally, a new structure type is presented: $Bi_8[Ta_2O_2Br_7]_2$, which contains the known square-antiprismatic Bi_8^{2+} ions and a new bromooxotantalate(V) ion.

[a] Institut für Anorganische Chemie der Rheinischen Friedrich-Wilhelm-Universität Bonn,
Gerhard-Domagk-Straße 1, 53121 Bonn, Germany
Fax: (internat.) + 49-228-735660
E-mail: j.beck@uni-bonn.de

Results and Discussion

Syntheses of $Bi(Bi_9)[NbCl_6]_3$ and $Bi_8[Ta_2O_2Br_7]_2$

A common method for synthesizing polycationic bismuth clusters is the crystallization as tetrachloroaluminates from NaCl/$AlCl_3$ melts. This involves the difficulty of separating the crystals from the solidified melt. Compounds containing polyatomic bismuth clusters are also available by chemical vapor deposition. We avoided a melt by applying relatively low reaction temperatures compared with those described in the literature.[9] The two compounds presented here can be seen as arising from comproportionation of elemental bismuth and the corresponding trihalide, since Bi_6Cl_7 or Bi_6Br_7 can be isolated as a subvalent intermediate, followed by a Lewis acid/base reaction of these intermediates with the respective metal halide.

$$9\ Bi + BiCl_3 + 3\ NbCl_5 \rightarrow Bi(Bi_9)[NbCl_6]_3$$

Even under optimized conditions the yields did not exceed 30%. Apparently, a multicomponent equilibrium involving Bi, $BiCl_3$, bismuth subhalides, transition metal halide and gas phase species is present, which prevents higher conversion rates. Removing the $Bi(Bi_9)[NbCl_6]_3$ crystals from the reaction mixture led to a second yield of about the same amount. Large pure samples are hard to obtain by this method. The bismuth subchloride Bi_6Cl_7 is formed as black crystals under the same conditions and must be separated mechanically. This is complicated by the various crystal forms of Bi_6Cl_7 which makes visual distinction from crystals of $Bi(Bi_9)[NbCl_6]_3$ difficult.

$Bi_8[Ta_2O_2Br_7]_2$ was obtained only in small yield by partial hydrolysis of $TaBr_5$. An overall reaction equation can be written, although the attempts to repeat the reaction with stoichiometric amounts of oxygen, introduced into the reaction system either via Ta_2O_5 or by short exposure of the reaction mixture to air were unsuccessful.

$$22\ Bi + 2\ BiBr_3 + 12\ TaBr_5 + 12\ H_2O \rightarrow 3\ Bi_8[Ta_2O_2Br_7]_2 + 24\ HBr$$

Crystal Structure of $Bi(Bi_9)[NbCl_6]_3$

$Bi(Bi_9)[NbCl_6]_3$ crystallizes isotypically to $Bi(Bi_9)[HfCl_6]_3$,[4] $Bi(Bi_9)[ZrBr_6]_3$,[9] and $Bi(Bi_9)[ZrCl_6]_3$.[10] All compounds that adopt this structure type are built of a close packing of two sorts of discrete molecular ions: triply μ_4-capped trigonal-prismatic Bi_9^{5+} cations and octahedral $[MX_6]^{2-}$ anions (Figure 1). The projection along the crystallographic *c*-axis (Figure 2) shows that each Bi_9 cluster is surrounded by six MX_6 octahedra in a coplanar arrangement. As in hexagonal closest sphere packing, six further anions are in a trigonal arrangement placed below and above. The hexahalometalate anions form wide channels that are centered around the cell edges and run perpendicular to the hexagonal plane. The channels are ca. 630 pm in diameter and are filled with columns of disordered Bi^+ ions (vide infra).

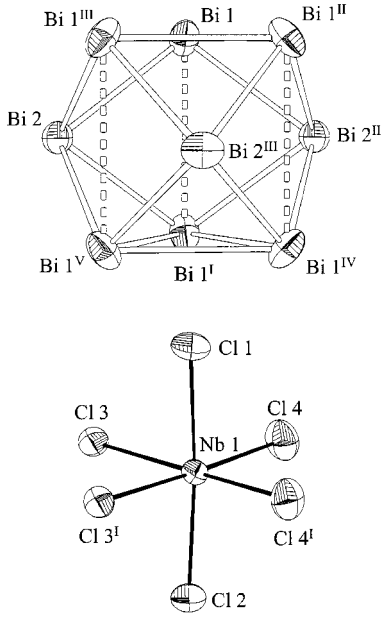

Figure 1. Bi_9^{5+} cluster and the $[NbCl_6]^{2-}$ ion in $Bi(Bi_9)[NbCl_6]_3$; displacement ellipsoids are scaled to enclose 50% probability density;[44] symmetry operations: I: *x*, *y*, 0.5 − *z*; II: 1 − *y*, *x* − *y*, *z*; III: 1 − *x* + *y*, 1 − *x*, *z*; IV: 1 − *y*, *x* − *y*, 0.5 − *z*, V: 1 − *x* + *y*, 1 − *x*, 0.5 − *z*; selected bond lengths [pm]: Bi(1)−Bi(2)/Bi(2)−Bi(1^I) 308.7(1), Bi(1)−Bi(2^{II})/Bi(2)−Bi($1^{III/V}$) 311.1(1), Bi(1)−Bi($1^{II/III}$) 324.3(1), Bi(1)−Bi(1^I) 373.8(1); Nb−Cl(1) 239.7(5), Nb−Cl(2) 239.8(5), Nb−Cl(3) 248.7(3), Nb−Cl(4) 234.8(3)

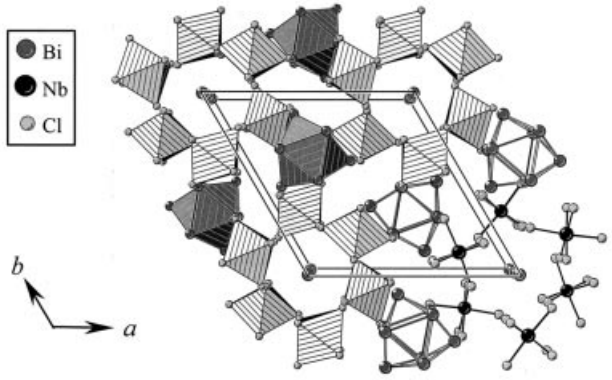

Figure 2. Unit cell of $Bi(Bi_9)[NbCl_6]_3$ in a perspective projection along the *c*-axis; the drawing combines shaded polyhedra and ball-and-stick models

The tri-capped trigonal-prismatic Bi_9^{5+} has crystallographic C_{3h} symmetry and is defined by two independent Bi atoms. Bi−Bi bonds, with the exception of the non-bonding prism edges (373.8 pm), have an average length of 314.7 pm. This agrees well with the literature values.[4] The difference between Bi−Bi bond lengths from a capping Bi(2) atom to the four corresponding Bi(1) atoms in the prism vertices is only 0.8%. This small irregular capping indicates only small distortions from the approximately fulfilled D_{3h} symmetry of the cluster ion.

Cl−Nb−Cl angles of the $[NbCl_6]^{2-}$ ion deviate by less than 3° from rectangularity; the Nb−Cl bonds, however, show considerable alternation in their lengths, between

234.8 and 248.7 pm. Both Cl(3) atoms of the $[NbCl_6]^{2-}$ ion, which have the longest Nb−Cl bonds, take a bridging position over edges of the cluster cation, with the shortest Bi−Cl distances of 333.5 pm. Distortions of the hexachloro metalate anions in this structure type from the ideal octahedral shape reflect the electrophilic properties of the Bi_9^{5+} clusters.

Disorder of the Bi^+ Ions in the Structure Type $Bi(Bi_9)[MX_6]_3$

Several crystal structures with a one-dimensional disorder of atoms or ions located in channels are known. $Bi_{5,6}Ni_5I$[22] contains double-walled channels of nickel and bismuth atoms. Their central axis is filled with a coaxial string of disordered Bi atoms that, statistically, occupy only every fifth possible site. Other examples include the compounds Th_7S_{12},[23] $K_2Sn_5Cl_{12}$ [24] and several apatite[25] and hollandite type structures.[26] With $Bi(Bi_9)[NbCl_6]_3$ the electron density along the *c*-axis is sufficient for only two additional Bi^+ ions per unit cell. X-ray experiments gave no direct evidence for disorder in the form of diffuse scattering. Precession photographs and imaging plate exposures did not show any continuous streaks in the reciprocal lattice along *c**.

The split-position model involves 14 closely neighbored atomic positions along one translation period on the sixfold axis in (0,0,*z*). Of the four independent split sites position C has the highest occupation factor (Figure 3). This marked preference might be due to the almost octahedral coordination with Cl atoms of the surrounding hexahalometalate(IV) ions (d_{Bi-Cl}: 3 × 320 pm, 3 × 337 pm). To measure the interaction between the various Bi(3) sites and the neighboring anions we calculated the electrostatic potential for a hypothetical atom in (0,0,*z*) using the program MAPLE (Madelung Part of Lattice Energy).[27] The results show only a very flat modulation of the potential in the center of the channel, while even small shifts of the dummy atom towards one of the $[NbCl_6]^{2-}$ octahedra increased its potential significantly (Figure 4). The tendency to localization on one particular split position is expected to be small. The closest distance between sixfold axes is 1377 pm, and no correlation can be expected for the parallel running chains.

The origin of the elongated displacement ellipsoids in the refinements with anisotropic displacement parameters was examined by low-temperature X-ray diffraction. One set of independent reflections was collected at 223 and 173 K. The temperature dependence of the mean-square displacement parameters of the disordered Bi(3) and of Bi(1), a fully occupied atom site making up the Bi_9 cluster, is represented in Figure 5. For a thermally vibrating atom one expects a linear decrease of the mean square displacements, to approximately zero when extrapolated to 0 K. Bi(1) shows such regular behavior, while Bi(3) behaves differently. While the unusual long axis of the displacement ellipsoid diminishes on decreasing temperature, the two symmetry-equivalent short axes perpendicular to the crystallographic *c*-axis, however, turned out to be temperature-independent. For both low-temperature data sets, difference Fourier maps

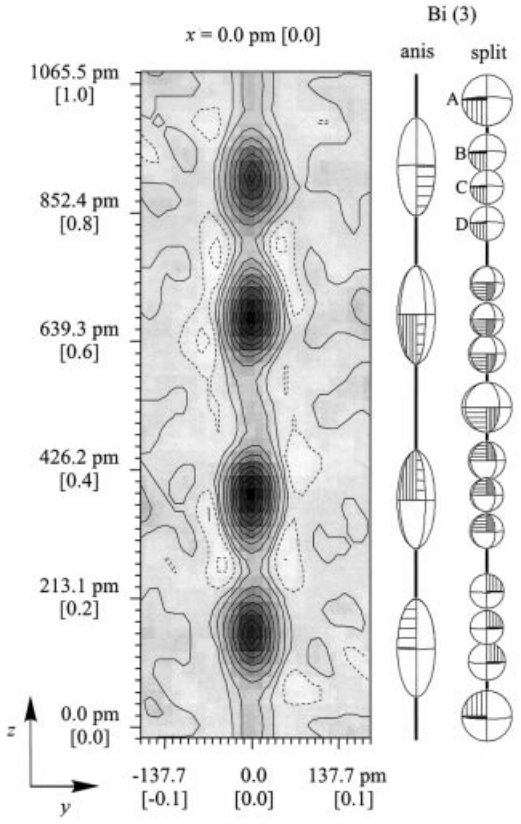

Figure 3. Difference Fourier electron density plot along the unit cell edge [001] in the structure of $Bi(Bi_9)[NbCl_6]_3$ − based on a structure model that was complete apart from the disordered Bi atoms in (0,0,*z*) and representations of the split positions and the disorder model for the Bi(3) site; displacement ellipsoids and spheres are scaled to enclose a 50% probability density

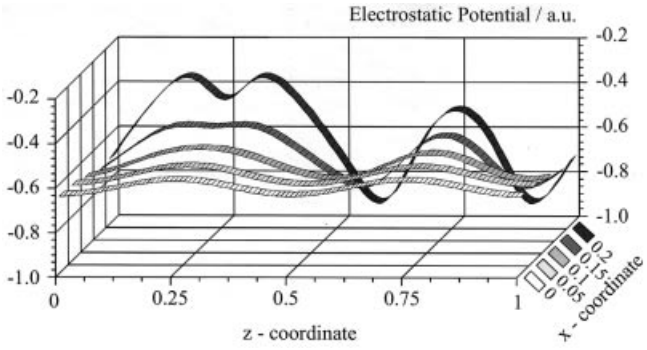

Figure 4. Electrostatic potential (arbitrary units) for a hypothetical atom on a site (0,0,*z*) under the influence of the anionic environment of $[NbCl_6]^{2-}$ ions in $Bi(Bi_9)[NbCl_6]_3$; since the dummy atom was assumed to be uncharged negative potentials indicate favorable positions for positively charged ions

show a contraction of the electron density maxima for the Bi(3) positions, but a diffuse density along the *c*-axis remains. Thus, elongation of the Bi(3) ellipsoids can not be attributed solely to a dynamical vibration phenomenon.

While previous structure determinations of compounds of this family[4,9] left it unclear whether the distribution of

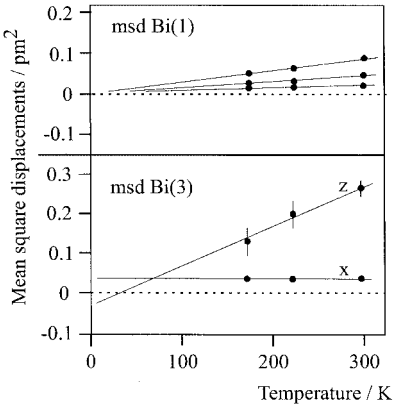

Figure 5. Temperature dependence of the mean square displacements of the atoms Bi(1) and Bi(3) in $Bi(Bi_9)[NbCl_6]_3$; errors of $\pm 3\sigma$ are indicated by vertical lines when bigger than the diameter of the dots

the disordered Bi ions should be interpreted as isolated Bi^+ ions or if two ions are associated in Bi_2^{2+} pairs with a bond length of ca. 300 pm, cationic Bi_2 dumbbells have been discovered in the phases $Bi_2M_4X_8$ (M = Al, Ga; X = S, Se).[12] The average Bi−Bi distances in the Bi_2^{4+} ions is 314 pm. Shorter Bi−Bi bonds are found in dibismuthanes with arene ligands, e.g. in Bi_2Ph_4 (d_{Bi-Bi} = 299 pm)[28] or in dibismuthenes ($d_{Bi=Bi}$ = 282 pm).[29] The presence of Bi_2^{2+} dumbbells may explain the distances (296 pm) between neighboring split atom positions in the ordered structure model of $Bi(Bi_9)[NbCl_6]_3$. The centers of gravity of these diatomic molecules are at (0,0,0) and (0,0,1/2). However, the intermolecular distance is only 237 pm, and only every second position can be statistically occupied by Bi_2^{2+}.

For $Bi_2[M_4X_8]$ (M = Al, Ga; X = S, Se) the Raman stretching vibration of the Bi_2^{4+} dumbbells is at 108 cm^{-1}.[12] Examination of $Bi(Bi_9)[ZrCl_6]_3$ and $Bi(Bi_9)[ZrBr_6]_3$ as easily obtainable model compounds for the structure type $Bi(Bi_9)[MX_6]_3$, and of Bi_6Cl_7, by IR and Raman spectroscopy show only a few lines in the region below 500 cm^{-1} {$Bi(Bi_9)[ZrCl_6]_3$: IR: $\tilde{\nu}$ = 289, 232, 162, 142, 112; Raman: $\tilde{\nu}$ = 224, 197, 158, 108, 93; $Bi(Bi_9)[ZrBr_6]_3$: IR: $\tilde{\nu}$ = 223, 189, 142, 108; Raman: $\tilde{\nu}$ = 170, 140, 106; Bi_6Cl_7: IR: $\tilde{\nu}$ = 422, 367, 212, 144, 107 cm^{-1}}. Comparison of $Bi(Bi_9)[ZrCl_6]_3$ and $Bi(Bi_9)[ZrBr_6]_3$ reveals a large drift for some of the IR absorption bands and some Raman lines. This indicates that the bands at 289, 232, 197, 162/158 cm^{-1} for $Bi(Bi_9)[ZrCl_6]_3$, and the bands at 223, 189, 170 cm^{-1} $Bi(Bi_9)[ZrBr_6]_3$ are attributable to vibration modes of the $[ZrX_6]^{2-}$ octahedra. The lines around 140 and 108 cm^{-1} appear for both compounds in the IR and Raman spectra but are also observed for Bi_6Cl_7. Since all three compounds contain Bi_9^{5+} clusters, these lines can, probably, be attributed to vibrations of the cluster ions. Distinct vibration bands attributable to Bi_2^{2+} groups are not present.

Neither of the two models, discrete Bi^+ ions or dinuclear Bi_2^{2+} ions, can be assigned on the basis of the present diffraction experiments and vibrational spectra.

Thermomagnetic Properties of $Bi(Bi_9)[NbCl_6]_3$

Analysis of the magnetic measurement unequivocally confirms the expected oxidation state of Nb^{IV}. The substance shows paramagnetic behavior, which is in contrast to the diamagnetic properties of $Bi(Bi_9)[HfCl_6]_3$ [4] and directly reflects the electronic state of the niobium atom. The effective magnetic moment at room temperature is well below the 1.72 B.M. for a spin-isolated single electron. Further, the simple Curie−Weiss law cannot be applied because the determined magnetic moment displays a distinct temperature dependency: its values increase from 0.99 at 76 K to 1.22 B.M. at 295 K per magnetic ion Nb^{IV} (Figure 6). Comparable behavior has been reported for other d^1-systems, e.g. in the compounds $M_2[NbCl_6]$ (M = Rb, Cs)[30] and $[N(C_2H_5)_4]_2[NbCl_6]$.[31]

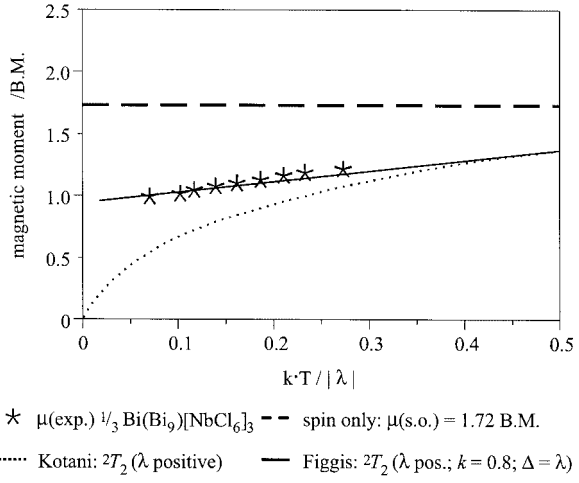

Figure 6. Temperature dependence of the effective magnetic moment of $Bi(Bi_9)[NbCl_6]_3$ scaled to a single magnetic Nb^{IV} ion; experimental data are set in relation to different theoretical approaches

The magnetic properties can be interpreted in terms of the models introduced by Kotani[32] and Figgis.[33] The effective magnetic moment arising from the $^2T_{2g}$ ground state of a transition metal complex ion in a centric symmetry ligand field depends upon several ligand field parameters: the spin-orbit coupling constant λ ($\lambda_{Nb^{IV}}$ = 750 cm^{-1} [34]), the orbital separation Δ between levels of the $^2T_{2g}$ term created by an axial ligand field, and the so-called orbital reduction factor k, which takes into consideration the delocalization of t_{2g} electrons into the orbitals of the ligand atoms.[35] The simplified Kotani model only takes into account the spin-orbit coupling, disregarding any distortion of the octahedral ions (k = 1 and Δ = 0 cm^{-1}). For the temperature dependence of the magnetic moments of $Bi(Bi_9)[NbCl_6]_3$ the best fit is reached in a model with Δ = 750 cm^{-1} and k = 0.8, reflecting the marked distortion of the $[NbCl_6]^{2-}$ polyhedra (Figure 6).

Crystal Structure of $Bi_8[Ta_2O_2Br_7]_2$

The structure contains square-antiprismatic Bi_8^{2+} clusters formerly known exclusively in $Bi_8[AlCl_4]_2$.[3] The coun-

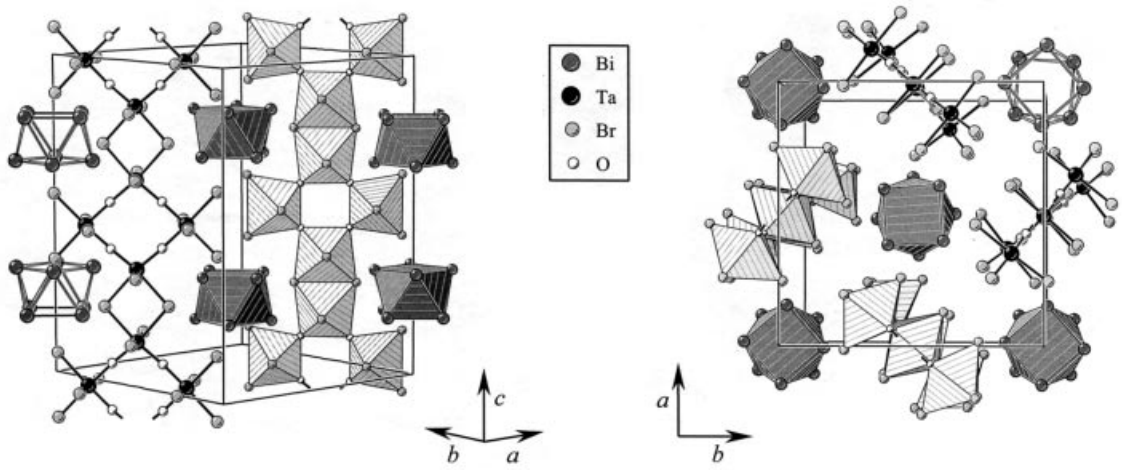

Figure 7. Unit cell of $Bi_8[Ta_2O_2Br_7]_2$ in two different views, along [110] and [001]; the drawing combines shaded polyhedra and ball-and-stick representations

terion is a novel, one-dimensional polymeric bromooxotantalate(v). Stacks of bismuth clusters and anionic chains are arranged in a tetragonal rod-packing along the crystallographic *c*-axis. Figure 7 shows two different views of the unit cell, along and perpendicular to the chains.

The Bi_8^{2+} cation has C_4 symmetry and is defined by two independent bismuth sites (Figure 8). The square faces are coplanar. Their twisting angle of 45.5° and the small difference in bond lengths [Bi(1) face: 312.6 pm; Bi(2) face: 311.7 pm] indicate only small distortions from the higher symmetrical point group D_{4d} (Table 1). Due to the lower charge per atom (*cpa*) the average Bi−Bi bond of 310.7 pm for Bi_8^{2+} (*cpa* = +0.25) is significantly shorter than the 314.7 pm observed for Bi_9^{5+} (*cpa* = +0.55). The cluster has to be considered as "naked" since the shortest anion−cation contacts are beyond 365 pm, and there are no intermolecular Bi−Bi distances shorter than 617 pm. The structure of the Bi_8^{2+} cluster ion in $Bi_8[Ta_2O_2Br_7]_2$ is very closely related to the cluster ion in $Bi_8[AlCl_4]_2$ [3,5,6] where Bi_8^{2+} has C_s symmetry and is generated by five crystallographically independent Bi atoms. There is a significant difference in the interionic intercations. In contrast to $Bi_8[Ta_2O_2Br_7]_2$ the shortest contacts between Bi atoms of neighboring Bi_8^{2+} ions in $Bi_8[AlCl_4]_2$ are only 390 and 410 pm, which indicate weak interactions between the clusters.

After $Te_4[Ta_2OBr_{10}]$[18] and $(NH_4)_2[Ta_3O_5Br_7]$,[36] $[Ta_2O_2Br_7]^-$ is only the third crystallographically characterized bromooxotantalate(v) reported. In contrast to $[Ta_2OBr_{10}]^{2-}$ ($Te_4[Nb_2OCl_{10}]$[37]) and $[Ta_3O_5Br_7]^{2-}$ {$(NH_4)_2[Nb_3O_5Cl_7]$[38]} no isostructural Nb/Cl analogue is known for $[Ta_2O_2Br_7]^-$. This anion consists of two symmetrically independent TaO_2Br_4 octahedra. Four vertex-sharing octahedra are connected by common oxygen atoms. The resulting tetrameric cyclic subunits are linked by common edges via four μ_2-Br atoms and form a one-dimensional polymeric anionic string (Figure 8). With Ta−O distances of 187 and 190 pm and Ta−O−Ta angles of 175.1° the oxygen bridges are nearly linear and symmetric. These

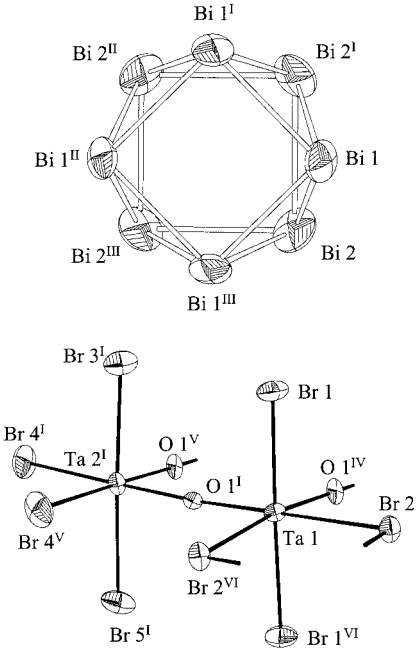

Figure 8. Bi_8^{2+} cluster and a section of the polymeric $[Ta_2O_2Br_7]^-$ ion in $Bi_8[Ta_2O_2Br_7]_2$; displacement ellipsoids are scaled to enclose 50% probability density;[44] symmetry operations: I: *y*, −*x*, *z*; II: −*x*, −*y*, *z*; III: −*y*, *x*, *z*; IV: 1 − *y*, *x*, *z*, V: *y*, −*x*, −*z*; VI: 1 − *x*, −*y*, *z*; selected bond lengths [pm]: Bi(1)−Bi(2) 308.7(3), Bi(1)−Bi(2^{I})/Bi(2)−Bi(1^{III}) 309.9(3), Bi(2)−Bi($2^{I/III}$) 311.7(2), Bi(1)−Bi($1^{I/III}$) 312.6(2); Ta(1)−O($1^{I/IV}$) 187(2), Ta(1)−Br(1) 2 × 248.5(2), Ta(1)−Br(2) 2 × 273.1(2), Ta(2)−O(1) 2 × 190(2), Ta(2)−Br(3^{I}) 249.5(4), Ta(2)−Br(4) 2 × 251.5(3), Ta(2)−Br(5) 253.5(4)

geometric parameters agree well with the Ta−O (188 pm) and linear Ta−O−Ta group in $[Ta_2OBr_{10}]^{2-}$.[18] Significantly shorter than the sum of the covalence radii of 209 pm,[39] the Ta−O bonds of both ions show strong indications of partial π-bonding. The four Ta−Br bonds of each tantalum atom in $[Ta_2O_2Br_7]^-$ vary substantially, between 248.5 and 273.1 pm for Ta(1), but only between 249.5 and 253.4 pm for Ta(2). This marked deviation reflects the

Table 1. Atomic coordinates, equivalent isotropic thermal displacement parameters B_{eq} [10^4 pm^2] and site occupation factors (*sof*) for the atoms in $Bi(Bi_9)[NbCl_6]_3$ and $Bi_8[Ta_2O_2Br_7]_2$; superscript sp refers to the split model, anis to the refinement with anisotropic displacement parameters

Atom	sof	*x*/*a*	*y*/*b*	*z*/*c*	B_{eq}
$Bi(Bi_9)[NbCl_6]_3$					
Bi(1)	1	0.51925(5)	0.21288(5)	0.07459(6)	3.38(2)
Bi(2)	1	0.48518(7)	0.37178(8)	0.25	3.16(2)
Nb(1)	1	0.6595(2)	0.7805(2)	0.25	1.98(3)
Cl(1)	1	0.4969(5)	0.8016(6)	0.25	3.6(1)
Cl(2)	1	0.8122(5)	0.7436(5)	0.25	2.89(8)
Cl(3)	1	0.5665(3)	0.6326(3)	0.0874(3)	2.47(6)
Cl(4)	1	0.7411(4)	0.9161(4)	0.0912(3)	3.57(7)
Bi(3A)^{sp}	0.07(2)	0	0	0	6(2)
Bi(3B)^{sp}	0.123(9)	0	0	0.087(2)	3.5(3)
Bi(3C)^{sp}	0.249(9)	0	0	0.142(1)	2.8(2)
Bi(3D)^{sp}	0.11(1)	0	0	0.201(2)	2.9(3)
Bi(3)^{anis}	0.495(4)	0	0	0.1389(6)	8.8(2)
$Bi_8[Ta_2O_2Br_7]_2$					
Bi(1)	1	0.15223(9)	0.0110(2)	0.1899(2)	5.47(5)
Bi(2)	1	0.1002(2)	0.1146(2)	0.3315(2)	6.57(5)
Ta(1)	1	0.5	0	0.13797(7)	1.13(3)
Ta(2)	1	0.12155(9)	0.34983(9)	0	1.43(3)
Br(1)	1	0.3862(2)	0.1276(2)	0.1495(2)	2.33(5)
Br(2)	1	0.5881(2)	0.0881(2)	0.25	1.66(6)
Br(3)	1	−0.0161(3)	0.2462(3)	0	2.86(8)
Br(4)	1	0.1944(2)	0.2558(2)	−0.1001(3)	3.22(7)
Br(5)	1	0.2571(3)	0.4605(3)	0	3.10(9)
O(1)	1	0.065(1)	0.425(1)	0.072(1)	1.4(3)

bridging character of Br(2) and the terminal character of all other Br atoms. In the dinuclear ion $[Ta_2OBr_{10}]^{2-}$ the static *trans* effect elongates the Ta−Br bonds *trans* to the allenic linear Ta=O=Ta group by 12 pm. This elongation, which is expected especially for the Br(4) atoms, is not present in $[Ta_2O_2Br_7]^-$.

Experimental Section

General: All compounds were handled in an argon-filled glove box. Reactions were carried out in evacuated and sealed glass ampoules (1.4 cm in diameter and 10−15 cm long), which were placed in horizontal tube furnaces. The ampoules were dried at 600 K before use. $BiCl_3$, $BiBr_3$, $NbCl_5$, and $TaBr_5$ were prepared from the elements as described[40] and sublimated under vacuum prior to use. Bismuth powder (Riedel−de Haën) was used without further treatment.

$Bi(Bi_9)[NbCl_6]_3$: A glass ampoule was filled under anhydrous conditions with Bi, $BiCl_3$ and $NbCl_5$ in the molar ratio 8:2:3 (310 mg in total). The ampoule was then evacuated, sealed and placed asymmetrically in a tube furnace that was heated to 550 K. The hot end of the ampoule contained the starting mixture; the empty end was at 535 K. Within several days black crystals formed on top of the mixed reagents and on the glass walls of the hot side of the ampoule. Even after several weeks, no conversion of more than about 30% was observed. When the product was mechanically removed and the remaining reaction mixture mortared, and again subjected to the same reaction conditions, a second crop of crystals of comparable yield was obtained. Larger crystals, suitable for X-ray investigations, formed at the glass walls of the warmer parts of the ampoule.

$Bi_8[Ta_2O_2Br_7]_2$: Traces of H_2O in the ampoule were responsible for the formation of $Bi_8[Ta_2O_2Br_7]_2$ in a reaction of Bi, $BiBr_3$ and $TaBr_5$ (molar ratio 8:2:3, 262 mg in total). A few black crystals of $Bi_8[Ta_2O_2Br_7]_2$ with the typical form of needles with a square cross section were obtained within 4 d in a temperature gradient from 570 to 550 K.

Bi_6Cl_7, $Bi(Bi_9)[ZrCl_6]_3$, and $Bi(Bi_9)[ZrBr_6]_3$: Used as reference samples for vibrational spectroscopy, were prepared from Bi and $BiCl_3$, $ZrCl_4$, and $ZrBr_4$, respectively, according to literature procedures.[3,9,10]

Crystal Structure Analyses: Since all compounds are moisture-sensitive the selected crystals were sealed under argon in glass capillaries. Crystallographic data and further details of the data collection and refinement (Table 2) and the positional parameters of the atoms (Table 1) are given here. Data collections were performed with a STOE IPDS image plate diffractometer equipped with a graphite monochromator and Mo-K_α radiation at room temperature and at low temperature using a cold nitrogen stream. All reflection intensities were corrected for Lorentz and polarization effects, and a numerical absorption correction was applied to each data set. The crystal shapes were optimized with the aid of the program HABITUS.[41] The program DIAMOND[26] was used for the graphical representations of the structures. Further details of the crystal structure analyses have been deposited at the Fachinformationzentrum Karlsruhe, 76344 Eggenstein-Leopoldshafen, Germany, and are available by quoting the authors, the literature citation and the deposit number CSD-410927 for $Bi(Bi_9)[NbCl_6]_3$, and CSD-410929 for $Bi_8[Ta_2O_2Br_7]_2$.

$Bi(Bi_9)[NbCl_6]_3$: In analogy to the isotypic compounds,[4,9] precession photographs showed the expected hexagonal crystal system with Laue class 6/*m*. The serial reflection condition 00*l*, only present for $l = 2n$, led to the space groups $P6_3/m$ or $P6_3$, of which the centrosymmetric space group was confirmed by structure analyses. A preliminary structure model, containing the atoms of the Bi_9 clusters and the $NbCl_6$ ions, was obtained by Patterson methods[42] and refined against F^2 by full-matrix least-squares calculations with anisotropic displacement parameters for all atoms.[43] A further difference Fourier calculation showed a high remaining electron density distributed along the edge of the unit cell at (0,0,*z*) with a diffuse maximum at $z/c \approx 0.1$ (Figure 3), which could be interpreted as two additional Bi^+ ions in each unit cell. Problems arise as the symmetry of the site 4*e* (0,0,*z*) generates four equivalent Bi atoms instead of two, and adjacent atoms come too close, with Bi−Bi distances just above 200 pm. Previously, a structure model implying disorder with four half-occupied Bi sites was used for $Bi(Bi_9)[HfCl_6]_3$ [4] and $Bi(Bi_9)[ZrBr_6]_3$.[9] As reported for these two crystal structures, refinement with anisotropic displacement parameters resulted in strongly elongated, "zeppelin-shaped" thermal ellipsoids for the Bi^+ ions. Further difference peaks between the positions of the disordered bismuth ions, especially on (0,0,0), allow refinement to a slightly modified structure model: four closely neighbored split positions in the interval (0,0,0) to (0,0,$^1/_4$) form a linear arrangement of partially occupied atom positions. Because of their proximity only isotropic displacement parameters could be refined for the split atoms. The site occupation factors have been refined without restraints and add up to 2.08(4) Bi atoms per unit

Table 2. Crystallographic data and details of structure refinement for the compounds $Bi(Bi_9)[NbCl_6]_3$ and $Bi_8[Ta_2O_2Br_7]_2$ (standard deviations in parentheses)

	$Bi(Bi_9)[NbCl_6]_3$	$Bi_8[Ta_2O_2Br_7]_2$
Empirical formula	$Bi_{10}Cl_{18}Nb_3$	$Bi_8Br_{14}O_4Ta_4$
Crystal system	hexagonal	tetragonal
Space group	$P6_3/m$	$P4/mnc$
Lattice constants	$a = 1377.1(2)$, $c = 1065.5(2)$ pm	$a = 1448.0(1)$, $c = 1830.6(2)$ pm
Unit cell volume	$V = 1749.8(3)\cdot10^6$ pm^3	$V = 3838.4(5)\cdot10^6$ pm^3
Number of formula units	$Z = 2$	$Z = 4$
Density (calculated)	$\rho = 5.706$ g·cm^{-3}	$\rho = 6.192$ g·cm^{-3}
Crystal dimensions	$0.095 \times 0.076 \times 0.475$ mm	$0.08 \times 0.09 \times 0.25$ mm
Diffractometer/radiation/temperature	Stoe Image Plate IPDS/Mo-K_α, $\lambda = 71.073$ pm/293 K	Stoe Image Plate IPDS/Mo-K_α, $\lambda = 71.073$ pm/293 K
Range of data collection	$9.5° \le 2\theta \le 56.3°$	$5.2° \le 2\theta \le 51.9°$
hkl range	$-18 \le h \le 18$; $-18 \le k \le 17$; $-13 \le l \le 13$	$-17 \le h \le 17$; $-17 \le k \le 17$; $-21 \le l \le 21$
Number of data collected	15926	27355
Number of unobserved reflections ($I \le 0$)	781	3297
Number of independent reflections/R_m	1471/0.098	1877/0.116
Number of reflections in least-squares	1471	1864; 13 reflections omitted
Absorption coefficient	$\mu = 523.9$ cm^{-1}	$\mu = 624.6$ cm^{-1}
Absorption correction/crystal shape[41]	numerical/11 faces	numerical/13 faces
Min./max. transmission T	0.0524/0.0788 anisotropic/isotropic split	0.0176/0.0600
Number of refined parameters	57/64	75
Ratio reflection/parameters	26/23	25
Extinction coefficient[43]	0.00351(6)/0.00351(6)	0.00011(2)
R values	0.068/0.066	0.085
$R(\|F\|)$ for all reflections	0.050/0.045	0.050
$R(\|F\|)$ [$F_o > 4\sigma(F_o)$]	1119/1119 reflections	988 reflections
$wR(F^2)$ for all reflections	0.068/0.066	0.118
Largest difference peak and hole [10^{-6} pm^{-3}]	+4.53 and −1.97/+3.40 and −1.93	+11.41/−2.32

cell. Although this alternative structure model slightly reduced the residual electron density, it had no significant effect on the overall quality of the refinement. The positions of the other atoms remained unchanged within their standard deviations.

$Bi_8[Ta_2O_2Br_7]_2$: Precession photographs showed the tetragonal crystal system with Laue class 4/*mmm*. Reflection conditions led to the space groups *P*4/*mnc* or *P*4*nc*, of which the centrosymmetric one was confirmed through structure analysis. The structure was solved by direct methods[42] and refined against F^2 by full-matrix least-squares calculations with anisotropic displacement parameters for all atoms.[43] A relatively large residual electron density was located at the origin of the unit cell. However, all attempts to include an atom at this position in the calculations did not enhance the quality of the structure refinement.

Magnetic Measurements: The thermomagnetic properties of $Bi(Bi_9)[NbCl_6]_3$ were determined on a sample (176 mg) of selected single crystals over the temperature range 76−295 K using a Faraday susceptometer. Measurements at several field forces showed no significant dependence. A diamagnetic correction was applied on the data. The purity of the sample was checked by powder X-ray diffractometry. Only a small impurity of Bi_6Cl_7 (ca. 5%) could be detected in the diffractogram.

Vibrational Spectroscopy: Infrared and Raman spectra were recorded using a Bruker IFS113V and a Bruker RFS100 spectrometer, respectively. For infrared spectroscopy, samples were prepared in a glove box as KBr discs. For Raman measurements, samples were finely ground with KBr in a mass ratio of 1:1 and placed in glass capillaries (1 mm diameter). We could not record a Raman spectrum of Bi_6Cl_7 as, even on cooling the sample capillary to 123 K, the compound decomposed in the laser beam.

Acknowledgments

Support of this work by the Deutsche Forschungsgemeinschaft and the Fonds der Chemischen Industrie is gratefully acknowledged.

Note added in proof (March 8, 2004): The synthesis and crystal structure of $Bi(Bi_9)[NbCl_6]_3$ was reported recently by: A. N. Kuznetsov, P. I. Naumenko, B. A. Popovkin, L. Kloo, *Russ. Chem. Bull.* **2003**, *52*, 2100−2104. The presence of Nb^{IV} was confirmed by the paramagnetic behaviour.

[1] J. D. Corbett, *Prog. Inorg. Chem.* **1976**, *21*, 129−158.
[2] A. Hershaft, J. D. Corbett, *J. Chem. Phys.* **1961**, *36*, 551−553; A. Hershaft, J. D. Corbett, *Inorg. Chem.* **1963**, *2*, 979−985; R. M. Friedman, J. D. Corbett, *Inorg. Chim. Acta* **1973**, *7*, 525−527.
[3] J. Beck, C. J. Brendel, L. Bengtsson-Kloo, B. Krebs, M. Mummert, A. Stankowski, S. Ulvenlund, *Chem. Ber.* **1996**, *129*, 1219−1226.
[4] R. M. Friedman, J. D. Corbett, *Inorg. Chem.* **1973**, *12*, 1134−1139.
[5] J. D. Corbett, *Inorg. Chem.* **1968**, *7*, 198−208.
[6] B. Krebs, M. Hucke, C. Brendel, *Angew. Chem.* **1982**, *94*, 453−454; *Angew. Chem. Int. Ed. Engl.* **1982**, *21*, 445−446.
[7] B. Krebs, M. Mummert, C. Brendel, *J. Less-Common Met.* **1986**, *116*, 159−168.

[8] H. von Benda, A. Simon, W. Bauhofer, *Z. Anorg. Allgem. Chem.* **1978**, *438*, 53−67.
[9] A. N. Kutznetsov, A. V. Shevel'kov, S. I. Troyanov, B. A. Popovkin, *Russ. J. Inorg. Chem.* **1996**, *41*, 920−923, translated from *Zh. Neorg. Khim.* **1996**, *41*, 958−961; A. N. Kuznetsov, A. V. Shevel'kov, B. A. Popovkin, *Russ. J. Coord. Chem.* **1998**, *24*, 861−866, translated from *Koord. Khim.*
[10] A. N. Kutznetsov, A. V. Shevel'kov, B. A. Popovkin, *Russ. J. Coord. Chem.* **1998**, *24*, 861−866, translated from *Koord. Khim.* **1998**, *24*, 919−924.
[11] S. Ulvenlund, K. Ståhl, L. Bengtsson-Kloo, *Inorg. Chem.* **1996**, *35*, 223−230.
[12] H. Kalpen, W. Hönle, M. Somer, U. Schwarz, K. Peters, H. G. von Schnering, R. Blachnik, *Z. Anorg. Allgem. Chem.* **1998**, *624*, 1137−1147.
[13] M. Ruck, *Z. Anorg. Allgem. Chem.* **1998**, *624*, 521−528.
[14] K. Wade, *Adv. Inorg. Chem. Radiochem.* **1976**, *18*, 1; K. Ichikawa, T. Yamamaka, A. Takamaken, R. Glaser, *Inorg. Chem.* **1997**, *36*, 5284.
[15] J. Corbett, P. A. Edwards, *J. Am. Chem. Soc.* **1977**, *99*, 3313−3317.
[16] T. F. Fässler, in *Metal Clusters in Chemistry* (Eds.: P. Braunstein, L. A. Oro, P. R. Raithby), Wiley-VCH, Weinheim, Germany, **1998**.
[17] J. D. Corbett, *Chem. Rev.* **1985**, *85*, 383−397; J. D. Corbett, *Struct. Bonding* ***1997****, 87*, 157.
[18] A. Hirsch, Z. Chen, H. Jiao, *Angew. Chem.* **2001**, *113*, 2916−2920.
[19] A. N. Kutznetsov, L. Kloo, M. Lindsjö, J. Rosdahl, H. Stoll, *Chem. Eur. J.* **2001**, *7*, 2821−2828.
[20] J. Beck, A. Fischer, *Z. Anorg. Allgem. Chem.* **1997**, *623*, 780−784.
[21] J. Beck, G. Bock, *Z. Naturforsch., Teil B* **1996**, *51*, 119−126.
[22] M. Ruck, *Z. Anorg. Allgem. Chem.* **1995**, *621*, 2034−2042.
[23] W. H. Zachariasen, *Acta Crystallogr.* **1949**, *2*, 288−291.
[24] H. P. Beck, H. Nau, *Z. Anorg. Allgem. Chem.* **1988**, *558*, 193−200.
[25] J. M. Hughes, M. Cameron, K. D. Crowley, *Am. Min.* **1990**, *75*, 295−304.
[26] J. E. Post, R. B. Von Dreele, P. R. Buseck, *Acta Crystallogr., Sect. B* **1982**, *38*, 1056−1065.
[27] R. Hübenthal, R. Hoppe, *MAPLE, Programm zur Berechnung von Kristallstrukturen, ECoN und Mefir*, University Gießen, Germany, **1993**.
[28] F. Calderazzo, R. Poli, G. Pelizzi, *J. Chem. Soc., Dalton Trans.* **1984**, 2365−2369.
[29] N. Tokitoh, Y. Arai, R. Okazaki, S. Nagase, *Science* **1997**, *277*, 78−80.
[30] V. T. Kalinnikov, N. P. Lipatova, O. D. Ubozhenko, A. A. Zharkikh, *Dokl. Akad. Nauk SSSR* **1973**, *210*, 107.
[31] G. W. A. Fowles, D. J. Tidmarsh, R. A. Walton, *Inorg. Chem.* **1969**, *8*, 631−638.
[32] M. Kotani, *J. Phys. Soc., Jpn.* **1949**, *4*, 293.
[33] B. N. Figgis, *Trans. Faraday Soc.* **1961**, *57*, 198; B. N. Figgis, J. Lewis, *Progr. Inorg. Chem.* **1964**, *6*, 37−239.
[34] T. M. Dunn, *Trans. Faraday Soc.* **1961**, *57*, 1441.
[35] M. Gerloch, J. R. Miller, *Progr. Inorg. Chem.* **1968**, *10*, 1−47.
[36] K.-P. Frank, Dissertation, University Tübingen, Germany **1983**.
[37] M. J. Collins, R. J. Gillespie, J. W. Kolis, J. F. Sawyer, *Acta Crystallogr., Sect. C* **1987**, *43*, 2033−2036.
[38] U. Reusch, E. Schweda, *Z. Anorg. Allg. Chem.* **1997**, *623*, 805−809.
[39] L. Pauling, *The Nature of the Chemical Bond*, Cornell University Press, Ithaca, USA, **1960**.
[40] G. Brauer, *Handbuch der präparativen Anorganischen Chemie*, 3rd ed., Ferdinand Enke Verlag, Stuttgart, Germany, **1981**.
[41] W. Herrendorf, H. Bärnighausen, *HABITUS, Program for Numerical Absorption Correction*, University Karlsruhe, Germany, **1993**.
[42] G. M. Sheldrick, *SHELXS-86, Program for Crystal Structure Determination*, University Göttingen, Germany, **1986**.
[43] G. M. Sheldrick, *SHELXL-93, Program for Crystal Structure Refinement*, University Göttingen, Germany, **1993**.
[44] *DIAMOND, Visual Information System for Crystal Structures*, Crystal Impact Comp., Bonn, Germany, **1996**.

Received September 11, 2003
Early View Article
Published Online March 31, 2004

